Chapter III: A cryptic Mesoarchean terrane in the basement to the Central African Copperbelt: U-Pb isotope evidence from detrital and xenocrystic zircons in the Muva and Katangan sequences*

C. RAINAUD[1], S. MASTER[1], R.A. ARMSTRONG[2] & L.J. ROBB[1]

[1]Economic Geology Research Institute/Hugh Allsopp Laboratory, School of Geosciences, University of the Witwatersrand, Pvt. Bag 3, WITS 2050, Johannesburg, South Africa.
[2]Research School of Earth Sciences, The Australian National University, Canberra, ACT 0200, Australia.

Abstract: In a study of the geochronology of the Katangan Sequence and its basement in the Central African Copperbelt (Rainaud et al., 1999), detrital and xenocrystic zircons from Muva quartzites and Katangan lapilli tuffs, were dated using the SHRIMP. A detrital population (dated between 3007 and 3031 Ma) and a group of xenocrystic zircons aged between 3169 and 3225 Ma provide the first evidence for the existence of a Mesoarchean basement beneath the Central African Copperbelt.

1. Introduction

The Central African Copperbelt, hosted by the Katangan Sequence, is situated in Zambia and the Katanga Province of the Democratic Republic of Congo (D.R.C.). The Katangan Sequence, which is subdivided into the Roan, Lower and Upper Kundelungu Supergroups, consists mainly of metasediments with minor mafic tuffs and sills (Figure 1). Its deposition took

* *This chapter appeared in Journal of the Geological Society, London, Vol. **160**, 2003, pp. 11-14*

place between 880 and 620 Ma (Armstrong et al., 1999; Cahen et al., 1984). The exposed basement to the Katangan Sequence consists of a Paleoproterozoic magmatic arc terrain dated at between 2050 Ma and 1800 Ma (Rainaud et al., 1999). On this basement the (as yet undated) Muva supracrustal succession of conglomerates, orthoquartzites and shales was deposited. This basement was then intruded by the 880 Ma Nchanga Granite, followed shortly by the deposition of the Katangan Sequence (Armstrong et al., 1999). To the west, the Katangan Sequence is flanked by the c. 1300-1000 Ma Kibaran Belt, which separates it from the Neoarchean rocks of the Kasai-Congo Craton (Cahen et al., 1984; Delhal, 1991; Tack et al., 1999).

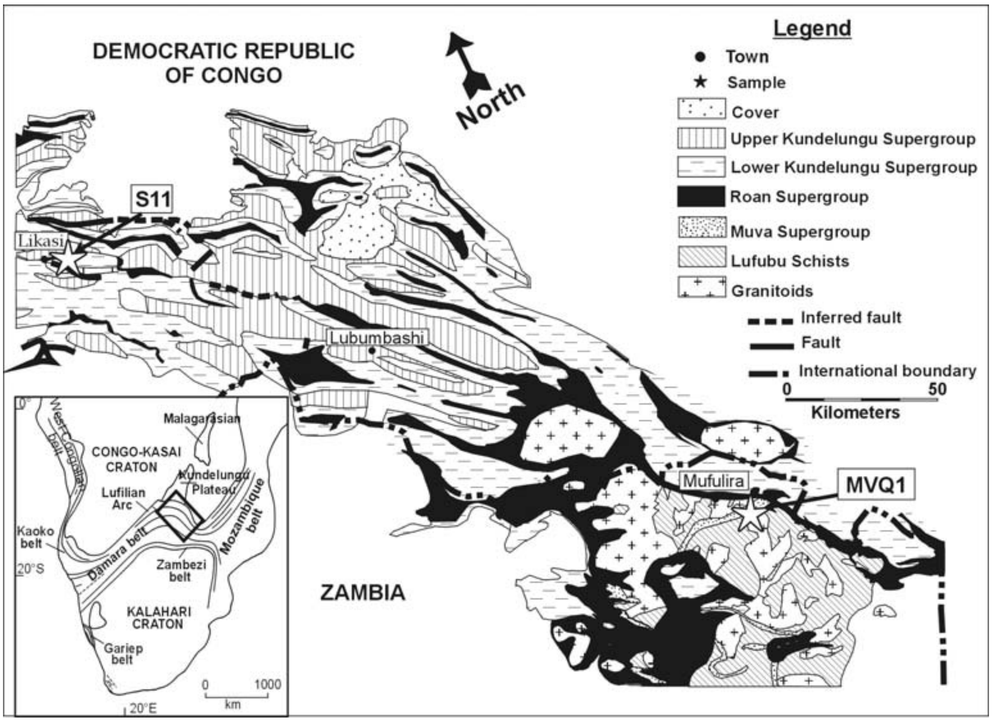

Figure 1. Simplified geological map of the eastern part of the Central African Copperbelt. After François, 1974.

2. Sampling

Detrital zircons were separated from a sample of crossbedded quartzite (MVQ1) from the Muva Supergroup, which was collected south of Mufulira (Zambia) at 21º12'E, 12º36'S. Numerous xenocrystic zircons were found in a lapilli tuff (S11) from the Mwashya Group in the upper part of the Roan Supergroup. This tuff was sampled at Shituru Mine (26º50'E, 11º01'S), near Likasi, in the central part of the Lufilian Arc (D. R. C.).

3. Analytical techniques

U-Pb analyses were performed on the SHRIMP I and II ion microprobes at The Australian National University, Canberra. The separation of zircons was carried out at the Hugh Allsopp Laboratory, Johannesburg, using conventional techniques. The SHRIMP analytical procedure used in this study is similar to that described by Claué-Long et al., (1995). Age calculations and plotting were done using Isoplot/Ex (Ludwig, 2000). Zircons from sample MVQ1 were randomly selected for analysis; in sample S11, more than 80% of all available zircons were analysed. In the following age interpretations only isotopic ratios that are 10% or less discordant were considered as reliable age indicators.

4. Detrital zircons

52 U-Pb analyses were carried out on 49 detrital zircons from sample MVQ1. Of these analyses, 49 were 10% or less discordant in terms of $^{207}Pb/^{206}Pb$ ages. The results are plotted on a concordia diagram in Figure 2, and the age distributions are shown on a histogram plot as an inset. The detrital zircons form several distinct populations, which range in age from 3180 to 1941 Ma. The youngest detrital zircons (22% of the population) form a cluster of ages peaking at 1990 Ma, but which range from 2099±15 Ma to

1941±40 Ma (which is the maximum age for the Muva quartzite) (Table 1). A second cluster of ages (39%) has a peak at about 2190 Ma, and ranges from 2297±20 to 2114 ±39 Ma. A third group of ages (6%) ranges from 2400±19 to 2371±17 Ma. A fourth group of zircons (23%) has ages which range from 2708±18 to 2463±25 Ma. This group has a bimodal distribution, with peaks at around 2500 Ma and 2700 Ma. There is a last group of zircons (8%) whose ages range from 3031±6 to 3007±15 Ma, with a peak at around 3020 Ma. Finally, the oldest detrital zircon is dated at 3180±12 Ma.

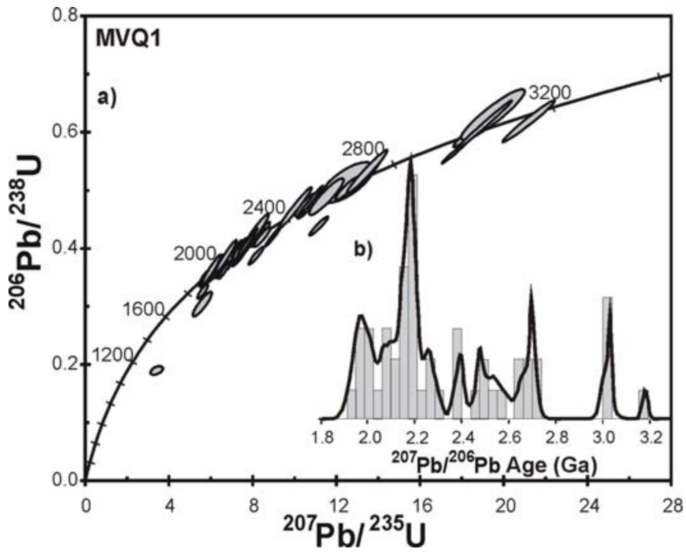

Figure 2. a) $^{206}Pb/^{238}U$ vs $^{207}Pb/^{235}/U$ concordia plot of ages (Ma) of detrital zircons from the Muva quartzite, sample MVQ1. b) Histogram plot showing the relative distribution of $^{207}Pb/^{206}Pb$ ages of the detrital zircons.

5. Xenocrystic zircons

Numerous zircons were found in a lapilli tuff (S11) from the Mwashya Group in the Katangan Sequence. Out of the 48 zircons analysed, 43 yielded $^{207}Pb/^{206}Pb$ ages that were 10% or less discordant (Figure 3). With the exception of two zircons which yielded very discordant $^{207}Pb/^{206}Pb$ apparent ages of 609 ± 288 Ma and681 ± 67 Ma (Table 2), all other zircons yielded ages greater than 880 Ma, the maximum age of the Katangan Sequence (Armstrong et al., 1999). Consequently the bulk of the zircon population from

Table 1. Summary of SHRIMP U-Th-Pb zircon results for sample MVQ1.

Grain. spot	U (ppm)	Th (ppm)	Th/U	Pb* (ppm)	$^{204}Pb/^{206}Pb$	f_{206} %	Radiogenic Ratios $^{206}Pb/^{238}U$	±	$^{207}Pb/^{235}U$	±	$^{207}Pb/^{206}Pb$	±	Ages (in Ma) $^{206}Pb/^{238}U$	±	$^{207}Pb/^{235}U$	±	$^{207}Pb/^{206}Pb$	±	Conc. %
1.1	132	188	1.42	84	0.00001	0.015	0.4770	0.0129	10.572	0.340	0.1607	0.0023	2514	56	2486	30	2463	25	102
2.1	413	168	0.41	175	0.00001	0.015	0.3935	0.0091	7.335	0.194	0.1352	0.0014	2139	42	2153	24	2166	18	99
3.1	343	186	0.54	134	0.00001	0.015	0.3803	0.0086	7.018	0.168	0.1339	0.0007	2078	40	2114	21	2149	10	97
3.2	388	36	0.09	153	0.00018	0.281	0.4014	0.0102	7.199	0.200	0.1301	0.0011	2176	47	2136	25	2099	15	104
4.1	143	55	0.38	66	0.00008	0.129	0.4282	0.0132	8.421	0.285	0.1426	0.0015	2297	60	2277	31	2260	19	102
5.1	102	97	0.96	48	0.00058	0.889	0.4027	0.0122	7.774	0.299	0.1400	0.0028	2182	56	2205	35	2227	35	98
7.1	140	139	0.99	84	0.00016	0.238	0.4844	0.0122	11.171	0.326	0.1673	0.0020	2546	53	2538	28	2531	20	101
8.1	167	40	0.24	67	0.00037	0.561	0.3947	0.0103	7.140	0.259	0.1312	0.0029	2145	48	2129	33	2114	39	102
9.1	768	132	0.17	461	0.00013	0.207	0.5659	0.0125	17.707	0.404	0.2270	0.0008	2891	52	2974	22	3031	6	95
10.1	118	82	0.70	65	0.00007	0.101	0.4729	0.0127	10.671	0.320	0.1637	0.0017	2496	56	2495	28	2494	18	100
11.1	225	180	0.80	102	0.00004	0.066	0.3879	0.0096	7.362	0.210	0.1376	0.0016	2113	45	2156	26	2198	20	96
12.1	366	180	0.49	147	0.00007	0.112	0.3902	0.0086	7.355	0.180	0.1367	0.0011	2124	40	2156	22	2186	14	97
13.1	114	91	0.79	46	0.00047	0.716	0.3533	0.0100	5.794	0.219	0.1190	0.0026	1950	48	1946	33	1941	40	101
14.1	286	78	0.27	127	0.00019	0.298	0.4231	0.0105	9.012	0.238	0.1545	0.0010	2275	48	2339	24	2396	11	95
15.1	219	120	0.55	97	0.00032	0.491	0.4028	0.0102	7.625	0.237	0.1373	0.0021	2182	47	2188	28	2193	27	100
16.1	216	193	0.90	93	0.00026	0.402	0.3726	0.0089	6.325	0.174	0.1231	0.0014	2042	42	2022	24	2002	20	102
17.1	132	149	1.13	59	0.00032	0.494	0.4019	0.0125	7.390	0.262	0.1334	0.0018	2178	58	2160	32	2143	24	102
18.1	316	237	0.75	179	0.00016	0.244	0.4821	0.0172	10.764	0.398	0.1619	0.0010	2536	75	2503	35	2476	10	102
19.1	203	170	0.84	88	0.00006	0.085	0.3681	0.0099	6.558	0.198	0.1292	0.0014	2020	47	2054	27	2087	19	97
20.1	189	158	0.83	104	0.00041	0.621	0.5041	0.0127	12.538	0.359	0.1804	0.0020	2631	55	2646	27	2656	18	99
21.1	392	356	0.91	176	0.00012	0.190	0.3789	0.0092	6.312	0.172	0.1208	0.0012	2071	43	2020	24	1968	17	105
22.1	217	144	0.66	102	0.00012	0.179	0.4104	0.0107	7.775	0.244	0.1374	0.0020	2217	49	2205	29	2195	25	101
23.1	227	182	0.80	99	0.00029	0.442	0.4083	0.0100	7.653	0.213	0.1359	0.0014	2207	46	2191	25	2176	19	101
24.1	62	89	1.44	41	0.00028	0.422	0.4905	0.0204	11.558	0.552	0.1709	0.0032	2573	89	2569	46	2567	32	100
25.1	86	39	0.45	37	0.00034	0.523	0.4021	0.0119	7.488	0.263	0.1351	0.0021	2179	55	2172	32	2165	27	101
26.1	563	197	0.35	311	0.00005	0.071	0.5186	0.0110	13.218	0.290	0.1849	0.0006	2693	47	2695	21	2697	6	100
27.1	435	161	0.37	176	0.00088	1.349	0.3914	0.0099	8.213	0.231	0.1522	0.0015	2129	46	2255	26	2371	17	90
28.1	266	162	0.61	134	0.00022	0.340	0.4408	0.0103	11.201	0.286	0.1843	0.0014	2354	46	2540	24	2692	13	88

Notes :
1. Uncertainties given at the one σ level.
2. f_{206} % denotes the percentage of ^{206}Pb that is common Pb.
3. Correction for common Pb made using the measured $^{204}Pb/^{206}Pb$ ratio.
4. For % Conc., 100% denotes a concordant analysis.

Table 1. Summary of SHRIMP U-Th-Pb zircon results for sample MVQ1.

							Radiogenic Ratios						Ages (in Ma)						
Grain. spot	U ppm	Th ppm	Th/U	Pb* ppm	$^{204}Pb/^{206}Pb$	f_{206} %	$^{206}Pb/^{238}U$	±	$^{207}Pb/^{235}U$	±	$^{207}Pb/^{206}Pb$	±	$^{206}Pb/^{238}U$	±	$^{207}Pb/^{235}U$	±	$^{207}Pb/^{206}Pb$	±	Conc. %
29.1	73	29	0.39	53	0.00021	0.317	0.6179	0.0229	21.235	0.825	0.2493	0.0020	3102	92	3149	38	3180	12	98
30.1	147	76	0.52	87	0.00025	0.382	0.5180	0.0147	13.291	0.420	0.1861	0.0020	2691	63	2701	30	2708	18	99
30.2	25	23	0.90	16	0.00215	3.287	0.5144	0.0226	12.559	0.825	0.1771	0.0077	2675	97	2647	64	2626	75	102
31.1	190	74	0.39	87	0.00015	0.234	0.4218	0.0105	8.309	0.231	0.1429	0.0014	2269	48	2265	25	2262	17	100
32.1	208	353	1.70	87	0.00053	0.812	0.3613	0.0107	6.117	0.230	0.1228	0.0024	1988	51	1993	33	1997	36	100
33.1	124	104	0.84	51	0.00032	0.490	0.3594	0.0105	5.967	0.206	0.1204	0.0018	1979	50	1971	30	1962	27	101
34.1	200	127	0.64	92	0.00012	0.180	0.4115	0.0109	7.707	0.222	0.1358	0.0011	2222	50	2197	26	2175	15	102
35.1	166	56	0.34	71	0.00019	0.297	0.4027	0.0120	7.616	0.247	0.1372	0.0013	2181	55	2187	30	2192	17	100
36.1	348	146	0.42	138	0.00013	0.195	0.3720	0.0082	6.544	0.158	0.1276	0.0010	2039	38	2052	21	2065	13	99
37.1	110	124	1.13	58	0.00037	0.570	0.4224	0.0110	8.492	0.253	0.1458	0.0017	2271	50	2285	27	2297	20	99
38.1	331	157	0.47	128	0.00017	0.268	0.3665	0.0096	6.683	0.191	0.1322	0.0012	2013	45	2070	26	2128	16	95
39.1	75	128	1.71	66	0.00035	0.532	0.6118	0.0246	18.867	0.802	0.2237	0.0021	3077	99	3035	42	3007	15	102
39.2	33	43	1.33	28	0.00011	0.166	0.6288	0.0284	19.535	1.002	0.2253	0.0044	3145	113	3069	51	3019	32	104
40.1	285	1298	4.56	70	0.00354	5.423	0.1970	0.0050	3.454	0.194	0.1272	0.0060	1159	27	1517	45	2059	85	56
41.1	266	463	1.74	98	0.00048	0.734	0.3304	0.0079	5.639	0.170	0.1238	0.0019	1841	38	1922	26	2011	28	92
42.1	259	142	0.55	157	0.00022	0.331	0.5309	0.0126	13.592	0.351	0.1857	0.0014	2745	53	2722	25	2704	13	102
43.1	187	105	0.56	90	0.00014	0.260	0.4314	0.0204	8.172	0.418	0.1374	0.0020	2312	92	2250	47	2195	26	105
44.1	307	189	0.62	100	0.00105	1.971	0.3091	0.0140	5.624	0.301	0.1319	0.0031	1737	69	1920	47	2124	42	82
45.1	221	129	0.58	90	0.00029	0.541	0.3673	0.0167	6.059	0.301	0.1197	0.0018	2017	79	1984	44	1951	27	103
46.1	144	168	1.17	98	0.00007	0.138	0.5327	0.0244	13.500	0.653	0.1838	0.0020	2753	103	2715	47	2688	18	102
47.1	143	70	0.49	60	0.00012	0.235	0.3888	0.0187	6.747	0.348	0.1259	0.0017	2117	87	2079	47	2041	25	104
48.1	406	222	0.55	183	0.00009	0.162	0.4101	0.0178	7.735	0.347	0.1368	0.0010	2216	82	2201	41	2187	13	101
49.1	263	100	0.38	183	0.00007	0.126	0.6114	0.0274	19.110	0.877	0.2267	0.0012	3076	111	3047	45	3029	9	102
50.1	154	115	0.74	85	0.00004	0.066	0.4718	0.0229	10.069	0.515	0.1548	0.0017	2491	101	2441	48	2400	19	104

Notes :
1. Uncertainties given at the one σ level.
2. f_{206} % denotes the percentage of ^{206}Pb that is common Pb.
3. Correction for common Pb made using the measured $^{204}Pb/^{206}Pb$ ratio.
4. For % Conc., 100% denotes a concordant analysis.

tuff sample is interpreted to be xenocrystic in origin. These zircons form several distinct age populations ranging from 1018±27 Ma to 3225±11 Ma. Some of these zircon populations have ages that overlap those from the detrital zircon population in the Muva quartzite. However, some groups from the detrital suite are not represented in the suite and vice versa. The xenocrystic suite include a population of Mesoproterozoic zircons which is completely absent from the detrital zircon population in the Muva quartzites. The youngest xenocrystic zircon population, comprising 5 zircons (12% of the 43 analyses used), is dated at between 1537±89 and 1018±27 Ma. A second group of 22 zircons (51%) has Paleoproterozoic ages between 2105±25 and 1791±21 Ma, with a peak at c. 1860 Ma. One zircon grain provides an age of 2624±9 Ma, while another is dated at 3021±34 Ma. Finally, there is a large group of 14 zircons (33%) which are dated at between 3225±11 and 3169±13 Ma.

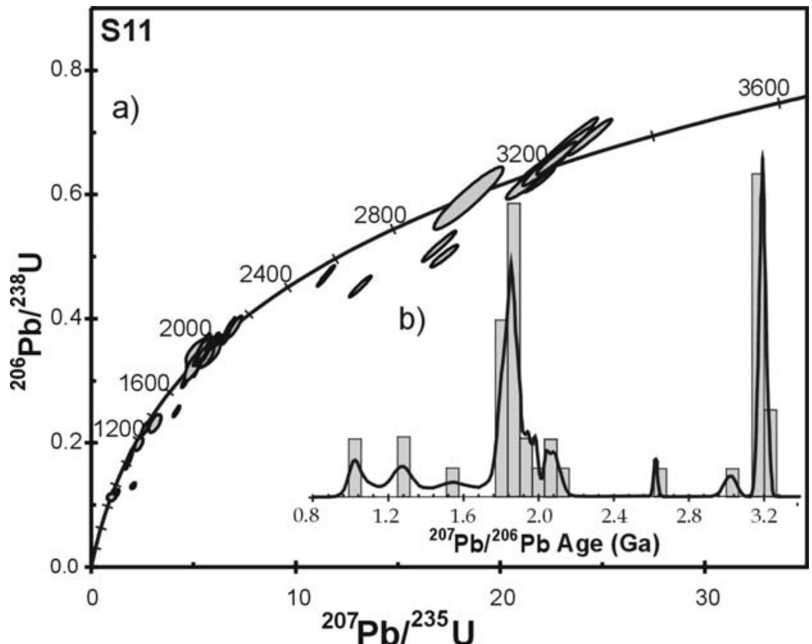

Figure 3. a) $^{206}Pb/^{238}U$ vs $^{207}Pb/^{235}/U$ concordia plot of ages (Ma) of inherited xenocrystic zircons from lapilli tuff (sample S11), Mwashya Group, Katangan Sequence. b) Histogram plot showing the relative distribution of $^{207}Pb/^{206}Pb$ ages of the xenocrystic zircons.

Table 2. Summary of SHRIMP U-Th-Pb zircon results for sample S11.

Grain. spot	U (ppm)	Th (ppm)	Th/U	Pb* (ppm)	$^{204}Pb/^{206}Pb$	f_{206} %	Radiogenic Ratios $^{206}Pb/^{238}U$	±	$^{207}Pb/^{235}U$	±	$^{207}Pb/^{206}Pb$	±	Ages (in Ma) $^{206}Pb/^{238}U$	±	$^{207}Pb/^{235}U$	±	$^{207}Pb/^{206}Pb$	±	Conc. %
1.1	269	288	1.07	105	0.00010	0.2	0.3224	0.0056	5.153	0.100	0.1159	0.0008	1801	28	1845	17	1894	12	95
2.1	194	197	1.02	79	0.00007	0.1	0.3348	0.0063	5.230	0.111	0.1133	0.0008	1862	31	1858	18	1853	13	101
3.1	271	231	0.85	54	0.00010	0.1	0.1730	0.0034	1.744	0.044	0.0731	0.0010	1029	19	1025	16	1018	27	101
4.1	215	149	0.69	82	0.00008	0.1	0.3397	0.0058	5.315	0.102	0.1135	0.0008	1885	28	1871	17	1856	12	102
5.1	94	91	0.97	38	0.00003	0	0.3315	0.0071	5.116	0.128	0.1119	0.0012	1846	35	1839	21	1831	19	101
6.1	152	122	0.80	66	0.00002	0	0.3703	0.0060	6.215	0.113	0.1218	0.0008	2031	28	2007	16	1982	11	103
7.1	176	222	1.26	76	0.00006	0.1	0.3380	0.0069	5.303	0.122	0.1138	0.0010	1877	33	1869	20	1861	15	101
8.1	93	100	1.07	78	0.00123	1.9	0.6363	0.0125	21.715	0.485	0.2475	0.0021	3174	49	3171	22	3169	13	100
9.1	89	72	0.81	73	0.00016	0.3	0.6489	0.0142	22.658	0.532	0.2532	0.0015	3224	56	3212	23	3205	10	101
10.1	102	68	0.66	44	0.00001	0	0.3768	0.0077	6.655	0.158	0.1281	0.0013	2061	36	2067	21	2072	17	100
11.1	159	116	0.73	60	0.00004	0.1	0.3299	0.0060	5.084	0.102	0.1118	0.0008	1838	29	1834	17	1829	12	101
12.1	122	69	0.57	41	0.00005	0.1	0.3060	0.0064	4.619	0.115	0.1095	0.0012	1721	32	1753	21	1791	21	96
13.1	95	80	0.84	76	0.00003	0	0.6326	0.0128	21.854	0.478	0.2505	0.0015	3160	51	3177	21	3188	10	99
14.1	136	163	1.20	118	0.00023	0.4	0.6422	0.0140	22.312	0.508	0.2520	0.0012	3198	55	3197	22	3197	7	100
15.1	88	79	0.90	71	0.00007	0.1	0.6246	0.0132	21.958	0.517	0.2550	0.0020	3128	53	3182	23	3216	13	97
16.1	130	169	1.30	118	0.00025	0.4	0.6601	0.0333	22.805	1.195	0.2506	0.0022	3268	131	3219	52	3188	14	103
17.1	226	118	0.52	44	0.00021	0.3	0.1841	0.0090	1.892	0.112	0.0745	0.0021	1090	49	1078	40	1056	59	103
18.1	146	111	0.76	55	0.00069	1.1	0.3310	0.0157	5.075	0.310	0.1112	0.0037	1843	76	1832	53	1819	62	101
19.1	80	58	0.73	67	0.00001	0	0.6740	0.0318	23.092	1.133	0.2485	0.0022	3321	124	3231	49	3175	14	105
20.1	73	51	0.69	59	0.00020	0.3	0.6498	0.0312	22.526	1.121	0.2514	0.0022	3228	123	3207	50	3194	14	101
21.1	90	76	0.84	73	0.00014	0.2	0.6379	0.0190	22.104	0.727	0.2513	0.0027	3181	75	3188	32	3193	17	100
22.1	53	79	1.51	17	0.00025	0.4	0.2394	0.0093	3.150	0.201	0.0954	0.0044	1384	48	1445	50	1537	89	90
23.1	145	133	0.92	116	0.00006	0.1	0.6202	0.0176	21.399	0.689	0.2503	0.0030	3111	70	3157	32	3186	19	98
24.1	78	148	1.89	23	0.00053	0.9	0.2064	0.0069	2.360	0.143	0.0829	0.0039	1210	37	1231	44	1267	94	96
25.1	225	89	0.40	54	0.00019	0.3	0.2310	0.0062	2.649	0.100	0.0832	0.0020	1340	32	1315	28	1273	46	105

Notes :

1. Uncertainties given at the one s level.
2. f_{206} % denotes the percentage of ^{206}Pb that is common Pb.
3. Correction for common Pb made using the measured $^{204}Pb/^{206}Pb$ ratio.
4. For % Conc., 100% denotes a concordant analysis.

Table 2. Summary of SHRIMP U-Th-Pb zircon results for sample S11.

Grain. spot	U (ppm)	Th (ppm)	Th/U	Pb* (ppm)	$^{204}Pb/^{206}Pb$	f_{206} %	Radiogenic Ratios $^{206}Pb/^{238}U$	±	$^{207}Pb/^{235}U$	±	$^{207}Pb/^{206}Pb$	±	Ages (in Ma) $^{206}Pb/^{238}U$	±	$^{207}Pb/^{235}U$	±	$^{207}Pb/^{206}Pb$	±	Conc. %
26.1	230	34	0.15	132	0.00007	0.1	0.5191	0.0158	17.067	0.551	0.2385	0.0018	2695	67	2939	31	3110	12	87
27.1	219	194	0.88	95	0.00012	0.2	0.3683	0.0090	6.045	0.163	0.1191	0.0011	2021	42	1982	24	1942	16	104
28.1	96	72	0.75	79	0.00015	0.2	0.6532	0.0255	22.561	0.940	0.2505	0.0027	3241	100	3208	41	3188	17	102
29.1	210	119	0.57	92	0.00013	0.2	0.3924	0.0108	7.061	0.229	0.1305	0.0018	2134	50	2119	29	2105	25	101
30.1	359	222	0.62	137	0.00014	0.2	0.3447	0.0093	5.235	0.153	0.1101	0.0009	1909	45	1858	25	1802	16	106
31.1	435	36	0.08	212	0.00007	0.1	0.4725	0.0107	11.523	0.275	0.1769	0.0009	2495	47	2566	23	2624	9	95
32.2	178	82	0.46	65	0.00030	0.5	0.3435	0.0100	5.693	0.213	0.1202	0.0024	1904	48	1930	33	1959	36	97
33.1	401	214	0.53	213	0.00041	0.5	0.4556	0.0111	13.197	0.341	0.2101	0.0013	2420	49	2694	25	2906	10	83
34.1	266	115	0.43	163	0.00012	0.2	0.5039	0.0113	17.321	0.430	0.2493	0.0020	2631	49	2953	24	3180	13	83
35.1	25	20	0.79	10	0.00079	1.2	0.3509	0.0165	5.492	0.554	0.1135	0.0095	1939	79	1899	91	1856	159	104
36.1	207	318	1.54	101	0.00020	0.3	0.3672	0.0090	5.592	0.166	0.1105	0.0016	2016	42	1915	26	1807	26	112
37.1	286	263	0.92	43	0.00027	0.5	0.1291	0.0028	1.107	0.044	0.0622	0.0019	782	16	757	21	681	67	115
38.1	92	61	0.66	12	0.00111	2	0.1229	0.0037	1.019	0.132	0.0602	0.0073	747	21	714	68	609	288	123
38.2	117	94	0.81	17	0.00001	0	0.1298	0.0033	1.281	0.054	0.0716	0.0022	787	19	837	24	974	63	81
39.1	321	349	1.09	142	0.00019	0.3	0.3622	0.0072	5.730	0.136	0.1148	0.0012	1992	34	1936	21	1876	20	106
40.1	18	2	0.10	12	0.00006	0.1	0.5951	0.0326	18.506	1.128	0.2256	0.0047	3010	133	3016	60	3021	34	100
41.1	95	67	0.71	38	0.00008	0.1	0.3515	0.0111	5.630	0.203	0.1162	0.0016	1942	53	1921	32	1898	25	102
42.1	1046	1125	1.08	178	0.00130	2	0.1409	0.0026	2.075	0.066	0.1068	0.0026	850	14	1141	22	1746	44	49
42.2	533	333	0.62	155	0.00018	0.3	0.2586	0.0054	4.197	0.105	0.1177	0.0013	1482	28	1673	21	1922	21	77
43.1	86	63	0.73	72	0.00001	0	0.6753	0.0207	23.380	0.757	0.2511	0.0018	3326	80	3243	32	3192	12	104
44.1	182	181	0.99	78	0.00012	0.2	0.3526	0.0079	5.493	0.158	0.1130	0.0017	1947	38	1899	25	1848	28	105
45.1	128	100	0.78	52	0.00030	0.5	0.3572	0.0097	5.459	0.185	0.1108	0.0019	1969	46	1894	30	1813	32	109
46.1	219	459	2.09	111	0.00012	0.2	0.3417	0.0073	5.368	0.139	0.1140	0.0014	1895	35	1880	22	1863	22	102
47.1	95	64	0.67	77	0.00016	0.2	0.6585	0.0172	22.815	0.640	0.2513	0.0018	3261	67	3219	28	3193	12	102
48.1	95	61	0.64	81	0.00001	0	0.6918	0.0188	24.458	0.706	0.2564	0.0018	3389	72	3287	29	3225	11	105
49.1	265	121	0.46	112	0.00009	0.1	0.3926	0.0093	6.809	0.176	0.1258	0.0010	2135	43	2087	23	2040	13	105
50.1	270	335	1.24	119	0.00091	1.4	0.3487	0.0069	5.471	0.144	0.1138	0.0017	1929	33	1896	23	1861	27	104

Notes :
1. Uncertainties given at the one s level.
2. f_{206} % denotes the percentage of ^{206}Pb that is common Pb.
3. Correction for common Pb made using the measured $^{204}Pb/^{206}Pb$ ratio.
4. For % Conc., 100% denotes a concordant analysis.

6. Provenance of zircons

The youngest xenocrystic zircons in the Katangan tuff (1018±27 to 1537±89Ma) span the age of the Kibaran granites (1375 to 1000 Ma; Tack et al., 1999), and indicates the presence of Kibaran magmatic rocks beneath the central part of the Lufilian Arc. The absence of Kibaran-aged zircons from the detrital population in the Muva quartzite (which is derived from a much wider area than that sampled by the tuff) indicates that the Muva quartzites were most probably deposited before 1537±89 Ma. The large population of Paleoproterozoic detrital and xenocrystic zircons, dated between 1791 and 2105 Ma, overlaps the time period (2050 to 1800 Ma) of the Ubendian magmatic arc terrain that constitutes the Bangweulu Block and the exposed basement in the Zambian Copperbelt (Cahen et al., 1984; Rainaud et al., 1999). A younger group of c. 1860 Ma xenocrystic zircons from the tuff is not represented in the detrital zircon population from the Muva quartzite. The 2297 to 2114 Ma detrital zircons (which are also absent from the xenocrystic suite) are from an unknown source, since there are no dated rocks of this age in the immediate vicinity. They may be derived from the Magondi Belt of Zimbabwe, which has been dated at between 2160±100 and 2120±40 Ma (Höhndorf and Vetter, 1999; Master, 1991; Schidlowski and Todt, 1998). The earliest Proterozoic suite of detrital zircons, dated at between 2400 and 2371 Ma, may have been derived from the Luiza metasediments in the Kasai region of the Congo, which have been dated at c. 2400 Ma (Cahen et al., 1984), or from the c. 2400 Ma granulites of the Kasai-Lomami complex (Delhal et al., 1986). The largely Neoarchean suite of detrital zircons, dated between 2710 to 2460 Ma, appears to have been derived mainly from the Kasai Craton in Congo, NE Angola and NW Zambia, where granites and migmatites have been dated at 2560 to 2540 Ma (Key and Armstrong, 2000), and where 2870 Ma leucogranites were overprinted at 2600 to 2007 Ma (Delhal, 1991). Neoarchaean rocks do not appear to be abundant in beneath the Lufilian Arc, since only one xenocrystic zircon of this age (2624±9 Ma) was found in the Katangan tuff. The most enigmatic zircons from both the detrital and xenocrystic suites are the >3000 Ma (Mesoarchean) grains which fall in two clusters at c. 3020 and 3200 Ma. In the whole of Central Africa, there are no rocks that have been dated at 3200 Ma, while only a few dates of c. 3000 Ma are known in widely separated regions such as Gabon (Cahen-Vachette et al., 1988), Zimbabwe (Cahen et al., 1984) and the northern Congo-Kasai Craton (Lavreau and Deblond, 2000).

7. Cryptic mesoarchaean terrane

There are no exposed rocks in the immediate vicinity of the Muva quartzites (or their proximal source regions) which are between 3300 and 3000 Ma in age. In eastern Zambia, Liyungu and Vinyu (1996) have obtained Pb model ages of 3047±130 Ma for zircons from the Chipata granite, and 2985±14 Ma for zircons from the Lutembwe granulite. The oldest dated rocks of the Kasai sector of the Archean Congo-Kasai craton of D.R.C. and NE Angola are c. 2900 Ma (Delhal, 1991). The greenstone belts and granites of Gabon, which constitute the western part of the Congo-Kasai craton, have been dated at 3100-2900 Ma (Cahen-Vachette et al., 1988). The Zimbabwe Archean craton consists mainly of 2900 to 2600 Ma granite-greenstone terranes, with only the southernmost Tokwe terrane containing older rocks dated at between 3500 and 2950 Ma (Kusky, 1998). The Archean Tanzanian craton is dated at between 2930 and 2530 Ma (Pinna et al., 1999). The detrital zircon population in the Muva quartzite has just one older 3180 Ma Mesoarchean zircon, and several zircons ranging from 3031 to 3007 Ma. By contrast, the Katangan tuff contains abundant older Mesoarchean xenocrystic zircons dated between 3225 and 3169 Ma, and only one younger zircon dated at 3021 Ma.

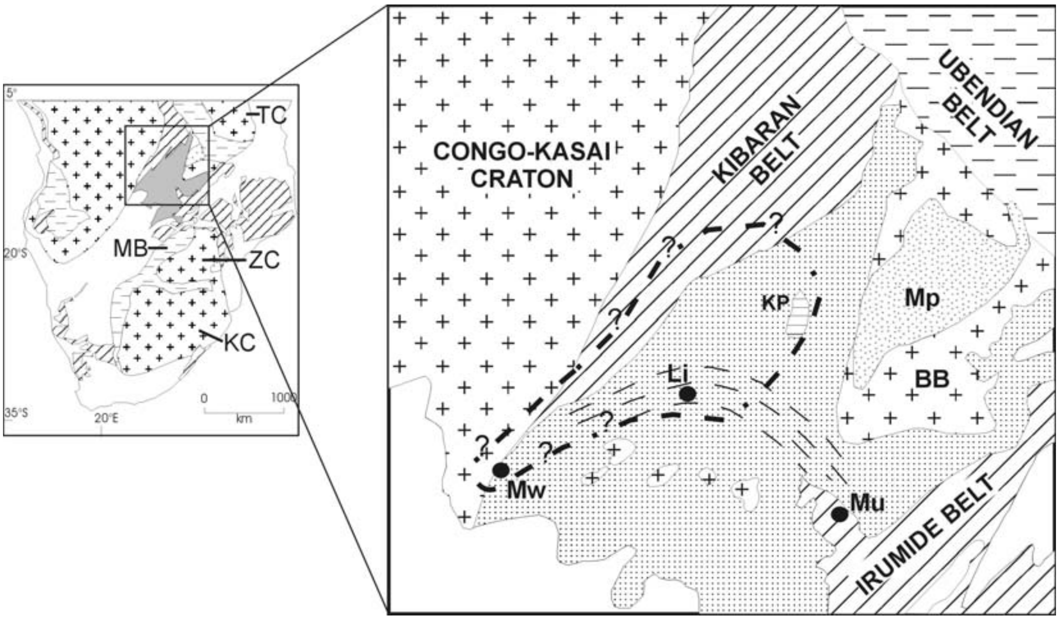

Figure 4. Sketch map showing the proposed extent of the Mesoarchean Likasi terrane (heavy dashes) beneath the Central African Copperbelt, relative to some of the important tectono-stratigraphic units of the region; i.e. the Lufilian Arc (light dashes extending from Mwinilunga [Mw] through Likasi [Li] to Mufulira [Mu]), the Neoarchean Congo-Kasai Craton, the Mesoproterozoic Kibaran and Irumide orogenic belts, the Paleoproterozoic Ubendian belt and Bangweulu block [BB], and the Muva Supergroup (Mp). The cluster of diamondiferous kimberlite pipes on the Kundelungu plateau is shown as KP .

The xenocrystic zircons originated from either the partially molten source region or the wallrocks in the path of ascent of the magmas that gave rise to the sampled Katangan tuffs. The lapilli tuffs at Shituru (which are interbedded with agglomerates) are the thickest and most proximal of all the tuffs in the Mwashya Group of the Katangan Sequence (Lefebvre, 1975). Therefore the xenocrystic zircons in these tuffs represent a sample of the crust beneath the central part of the Lufilian Arc, which is buried under the tectonically thickened Katangan Sequence. The abundance of c. 3200 Ma xenocrystic zircons in this tuff (32% of the total population) indicates that a part of the crust beneath the central Lufilian Arc is a c. 3200 Ma terrane that we propose to call the Likasi Terrane. The almost total absence of ages ranging from 2700 to 2500 Ma in the xenocrystic zircon population (which are abundant in the detrital zircon population) implies a lack of Neoarchean crust in the Likasi Terrane. The bulk of the remaining crust is of Palaeoproterozoic (Ubendian) age, between 2100 and 1800 Ma. There is also evidence from these xenocrystic zircons of Kibaran-aged crust (1300 to 1000 Ma) in this region. Because only a single c. 3200 Ma detrital zircon was found in the Muva quartzite, it appears that the 3200 Ma crust might have been poorly exposed at the surface, which was dominated by the c. 2000 Ma Ubendian crust. The 3200 Ma crust may have been more abundant at mid- or deep crustal levels beneath the Lufilian Arc. The xenocrystic and detrital zircons from the Katangan tuffs and Muva quartzites provide the only direct evidence for the existence of this cryptic Mesoarchean crust beneath the Katangan Sequence. The occurrence of diamonds in the kimberlites of the Kundelungu Plateau to the north of the Lufilian Arc (Demaiffe et al., 1991) may be an indirect indication of the presence of an Archean crust beneath the Katangan of Central Africa. In addition to mantle xenoliths, the Kundelungu kimberlites also contain undated crustal gneiss and mica-schist xenoliths, some of which may be samples of the cryptic Likasi Terrane. In the northwestern corner of Zambia, near Mwinilunga, close to the borders with Angola and D.R.C., Neoarchean foliated granites dated at 2538±10 Ma contain xenocrystic inherited zircons which give a mixture of ages as old as 3154 Ma (Key and Armstrong, 2000). This indicates that the c. 3200 Ma Likasi Terrane may have extended towards the southwest from the Likasi area to the Mwinilungu area, over a distance of about 300 km (Figure 4). If the 3154 Ma xenocrystic zircons of Mwinilunga are derived from the Likasi Terrane, it implies that the latter was an integral part of the Kasai-Congo craton by the latest Archean. It is further suggested that the Likasi Terrane was accreted onto the Kasai-Congo craton before 2538 Ma, and that this collisional event may have been responsible for some of the granulite-facies metamorphism in the southeastern Kasai-Congo craton.

8. References

Armstrong, R. A., Robb, L. J., Master, S., Kruger, F. J. and Mumba, P. A. C. C., 1999, New U-Pb age constraints on the Katangan Sequence, Central African Copperbelt: Journal of African Earth Sciences, v. 28(4A), p. 6-7.

Caen-Vachette, M., Vialette, Y., Bassot, J. -P. and Vidal, P., 1988, Apport de la géochronologie isotopique à la connaissance de la géologie gabonaise: Chronique de la recherche minière, v. 491, p. 35-54.

Cahen, L., Snelling., N. J., Delhal, J., Vail, J. R., Bonhomme, M. and Ledent, D., 1984, The Geochronology and Evolution of Africa: Oxford, 512 p.

Claué-Long, J. C., Compston, W., Roberts, J. and Fanning, C. M., 1995, Two carboniferous ages: a comparison of SHRIMP zircon dating with conventional zircon ages and $^{40}Ar/^{39}Ar$ analysis: Geochronology Time Scales and Global Stratigraphic Correlation, SEPM Special Publication No 54, p. 1-21.

Delhal, J., Deutsch, S. and Denoiseux, B., 1986, A Sm-Nd isotopic study of heterogeneous granulites from the Archean Kasai-Lomami gabbro-norite and charnockite complex (Zaire, Africa): Chemical Geology, v. 57, p. 235-245.

Delhal, J., 1991, Situation géochronologique 1990 du Précambrien du Sud-Kasai et de l'Ouest-Shaba.: Tervuren, Musée royal d'Afrique centrale, Annual report 1990, p 119-125.

Demaiffe, D., Fieremans, M. and Fieremans, C., 1991, The kimberlites of Central Africa: a review, *in* Kampunzu, A. B. and Lubala, R.T., eds., Magmatism in Extensional Structural Settings: The Phanerozoic African Plate: Berlin, Springer, p. 537-559.

François, A., 1974, Stratigraphie, tectonique et minéralisations dans l'Arc cuprifère du Shaba (République du Zaïre), *in* Bartholomé, P., ed., Gisements stratiformes et provinces cuprifères: Société Géologique de Belgique, p. 79-101.

Höhndorf, A. and Vetter, U., 1999, The Sanyati Ore Deposits in Zimbabwe: Pb- isotopic investigation of sulfide and oxide ores: Zeitschrift für angewande Geologie, v. 45 (1), p. 11-13.

Key, R. M. and Armstrong, R. A., 2000, Geology and geochronology of pre-Katangan igneous and meta-igneous rocks north of the Lufilian Arc in northwest Zambia: Journal of African Earth Sciences, v. 31, p. 36-37.

Kusky, T. M., 1998, Tectonic setting and terrane accretion of the Archean Zimbabwe craton: Geology, v. 26, p. 163-166.

Lavreau, J. and Deblond, A., 2000, Geological and chronological setting of the greenstone belts of the northern Congo Craton: Journal of African Earth Sciences, v. 30, p. 53.

Lefebvre, J. J., 1975, Les roches ignées dans le Katangien du Shaba (Zaïre). Le district du cuivre: Annales de la Société Géologique de Belgique, v. 98, p. 47-73.

Liyungu, A .K. and Vinyu, M. L., 1996, Constraints on the timing of the high grade Lutembe quartz-feldspathic granulite, charnockitic enderbite and the relationship to the Chipata granite in the Mozambique Belt, *in* Kamona, A. F., Tembo, F., Mapani, B. S. E. eds., Abstracts Volume, First International Field Conference of IGCP 363 Palaeoproterozoic of Sub-Equatorial Africa, 14-30 September, 1996, Zambia-Zimbabwe. Lusaka, Geol. Soc. Zambia, p. 19.

Ludwig, K. R., 2000. Users Manual for Isoplot/Ex version 2.3, a geochronological toolkit for Microsof Excel. Berkeley Geochronology Center, Special publication No. 1a.

Master, S., 1991, Stratigraphy, tectonic setting, and mineralization of the early Proterozoic Magondi Supergroup, Zimbabwe: a review: Economic Geology Research Unit Information Circular, Department of Geology, University of the Witwatersrand, Johannesburg, No. 238, 75 pp.

Pinna, P., Cocherie, A., Thieblemont, D., Jezequell, P.and Kayagoma, E., 1999, The Archean evolution of the Tanzanian craton (2.93-2.53 Ga): Journal of African Earth Sciences, v. 28, p. 62-63.

Rainaud, C., Armstrong, R. A., Master, S. and Robb, L. J., 1999, A fertile Palaeoproterozoic magmatic arc beneath the Central African Copperbelt, Mineral deposits: processes to processing: London, *in*: Stanley, C.J. et al. eds. Mineral Deposits: Processes to Processing, Volume 2: A. A. Balkema, Rotterdam, p. 1427-1430.

Schidlowski, M.and Todt, W., 1998, The Proterozoic Lomagundi carbonate province as a paragon of a 13C- enriched carbonate facies: Geology, radiometric age and geochemical significance: Chinese Science Bulletin, v. 43 (supplement), p. 114.

Tack, L. F. -A., M., Wingate, M. and Deblond, A., 1999, Critical assessment of recent unpublished data supporting a single and united geodynamic evolution of the Sao Francisco-Congo-Tanzania cratonic blocks in the Rodinia configuration: Journal of African Earth Sciences, v. 28, p. 75-76.